Strong-field photoionization by ultrashort low-frequency pulses

K. Babiarz,[1] A. Raczyński,[2,*] and J. Zaremba[2]
[1]*Katedra Podstaw Teoretycznych Nauk Biomedycznych i Informatyki Medycznej, Akademia Medyczna im. L. Rydygiera, ul. Skłodowskiej-Curie 9, 85-094 Bydgoszcz, Poland*
[2]*Instytut Fizyki, Uniwersytet Mikołaja Kopernika, ul. Grudziądzka 5, 87-100 Toruń, Poland*
(Received 23 February 2001; published 10 September 2001)

Photoionization in the regime of the barrier suppression is investigated within a three-dimensional, fully quantum-mechanical, time-dependent model. It is shown how a structure is formed in the envelope of the above threshold ionization spectra, for energies smaller than the ponderomotive potential. A correspondence between this structure and the shape of the initial-state decay curve, as well as the radial distribution of the electron wave packet, is proven.

DOI: 10.1103/PhysRevA.64.045401 PACS number(s): 32.80.Rm, 32.80.Gc, 32.80.Qk

Though our understanding of many aspects of the multiphoton ionization in strong laser fields is already quite good (e.g., Refs. [1,2]), some details of the dynamics of the process still need clarification. Further investigations are required, in particular, in the cases of very short and intense laser pulses (e.g., Ref. [3]), in the regimes of parameters in which the process changes its character and requires a description in terms of a new mechanism. Important examples are the situations in which the above threshold ionization (ATI) *sensu stricto* turns into tunneling or when tunneling turns into the ionization through the barrier suppression [2,4]. Then high maxima may appear in the decay curve of the initial state and the envelope of the ATI peaks may have local minima. In those circumstances, the two powerful theoretical tools applied to interpret strong-field effects, namely the usual Keldysh-Faisal-Reiss (KFR) approach [5] and the quasistatic model (see Ref [6] and the references therein), may no longer be reliable and their predictive power is then limited. The KFR formulas give the ionization rate, which is an adequate notion if the depletion of the subspace of discrete states is more or less exponential. The KFR model also assumes that the process takes a long time compared with the optical cycle, so the peaks in the photoelectron spectrum are much more narrow than the photon energy. This approach has already been generalized to account for rescattering [7,8], which must be considered if we want to interpret the high-energy part of the spectrum [energies being a few multiples of the ponderomotive potential—high-order above threshold ionization (HATI)], in particular the so-called plateaux. However, this method cannot be used in the case of short and strong low-frequency pulses, such that a large part of the population is first quickly transferred to the continuum and may later return to the initial state. As to the quasistatic model, it is in fact a not completely coherent combination of a picture of an electron tunneling through a potential barrier (with a time-dependent rate changing in the rhythm of the field) and that of a liberated electron evolving, in the simplest case, according to the Newton equations. In this approach, rescattering, which implies an existence of local minima in the decay curve, is thus not described quantum mechanically and is absent from the tunneling part of the model, in which the decay probability is a nonincreasing function of time. Within this model, having taken rescattering into account, one can explain the existence of the high-energy part of the photoelectron spectra [6,9–11] and some aspects of the high-harmonic generation (see Ref. [2] and the references therein), but not all the details of the spectra. Of course, the works based on a numerical integration of the Schrödinger equation [11] supply the detailed information on the dynamics, but they require a serious computational effort.

In the present paper, we will theoretically investigate the dynamics of the photoionization on the border between the tunneling and the barrier suppression regimes, due to very short pulses. We will use the tool discussed and applied in our previous work [12], which may be considered a time-dependent version of the KFR approach. In particular, the model accounts for rescattering and we will show that it predicts a significant nonmonotonic depletion of the initial state and minima in the envelope of the ATI peaks, in particular, in its low-energy part. We will give a many-sided picture of the process by presenting the decay curve of the initial state and the photoelectron spectra, as well as the radial probability distribution of the ejected electron shown at different stages of their formation.

The applied model has been presented in detail in Ref. [12]. We consider an atomic system with a single active electron. The space of the atomic states consists of a single discrete state $|1\rangle$ of energy E_1 and zero angular momentum and of the continuum states $|\mathbf{k}\rangle$ of energy $\epsilon_{\mathbf{k}}=(1/2)k^2$. The atom is irradiated by a linearly polarized laser pulse with vector potential $\mathbf{A}(t)=A(t)\hat{\mathbf{e}}$. The interaction Hamiltonian in the velocity gauge is $V=\mathbf{A}\cdot\mathbf{p}$ The aim is to calculate the time-dependent nondecay amplitude $a(t)\exp(-iE_1t)$ and the time-dependent ionization amplitude $b_{\mathbf{k}}(t)$.

The bound-continuum coupling is assumed in the form

$$|(\mathbf{e}\cdot\mathbf{p})_{1\mathbf{k}}|^2=\frac{3}{4\pi}C^2k^2\exp(-\gamma\epsilon_{\mathbf{k}})(\mathbf{e}\cdot\hat{\mathbf{k}})^2, \tag{1}$$

which gives an account of a proper threshold behavior in the case of short-range binding potentials ($|(\mathbf{e}\cdot\mathbf{p})_{1\mathbf{k}}|^2k^2dk/d\epsilon_{\mathbf{k}}\sim k^3\sim\epsilon_{\mathbf{k}}^{3/2}$ - Wigner power law [13]). The exponential function overestimates the rate of disappearing of the matrix el-

*Email address: raczyn@phys.uni.torun.pl

ements for $k\to\infty$. Note, however, that we will be concerned with neither threshold effects nor extremely large energies, so the choice of the model coupling should not limit the generality of our conclusions, while the model allows us to perform some integrals analytically. Below we take the following values of the model parameters: $C^2=9.184$ a.u., $\gamma=18.14$ a.u., and $E_1=-0.027\,565\,4$ a.u.; they correspond to the negative hydrogen ion. An electron in such an ion was often described as bound by a contact potential $V(r)=(2\pi/\zeta)\delta(\mathbf{r})(\partial/\partial r)r$ (see Refs. [12,14] and the references therein), where $E_1=-\zeta^2/2$. Such a potential yields a power dependence of the bound-continuum matrix elements instead of an exponential dependence of our model but a qualitative behavior of the two models (the threshold behavior, the position, and the height of the maximum) is similar.

The continuum-continuum coupling is taken, in the spirit of the KFR approach, as for free particles, i.e., $(\mathbf{e}\cdot\mathbf{p})_{\mathbf{k}\mathbf{k}'}=\mathbf{e}\cdot\mathbf{k}\delta(\mathbf{k}-\mathbf{k}')$. The scattering states are thus approximated by free-particle functions. An implicit consequence, common for all the works within the KFR family, is that the bound state is not exactly orthogonal to the continuum states. In our model, rescattering is taken into account because a multiple return to the initial state is allowed. Note that in our fully quantum model, the interference of the parts of the wave packet running in opposite directions is taken into account.

If we now project the Schrödinger equation onto the states $|1\rangle$ and $|\mathbf{k}\rangle$ we obtain a set of coupled equations for the amplitudes $a(t)$ and $b_{\mathbf{k}}(t)$. The equation for the latter amplitude is formally integrated and inserted into the equation for $a(t)$. As a consequence, the nondecay amplitude can be shown to satisfy an integrodifferential equation

$$\dot{a}(t)=-\int_0^t K(t,t')\,a(t')dt'. \tag{2}$$

The kernel $K(t,t')$ may, due to our choice of the bound-continuum coupling, be expressed in an analytical form

$$K(t,t')=3C^2\sqrt{\frac{\pi}{2}}A(t)A(t')e^{iE_1(t-t')}\left(\frac{1}{(\gamma+i\tau)^{5/2}}-\frac{G^2}{(\gamma+i\tau)^{7/2}}\right)\exp\left(-\frac{G^2}{2(\gamma+i\tau)}\right), \tag{3}$$

with $G=G(t,t')=\int_{t'}^t A(\tau)d\tau$. The ionization amplitude $b_{\mathbf{k}}(t)$ can be expanded into the spherical harmonics: $b_{\mathbf{k}}(t)=\Sigma_{l=0}^{\infty}b_l(k,t)Y_{l0}(\hat{\mathbf{k}})$, where

$$b_l(k,t)=\sqrt{3(2l+1)}(-i)^l Ck\exp[-\tfrac{1}{4}\gamma k^2-i\epsilon_{\mathbf{k}}t]\times\int_0^t A(t')\exp[i(\epsilon_{\mathbf{k}}-E_1)t']\times j_l'[kG(t,t')]a(t')dt', \tag{4}$$

with j_l' being the derivative of the half-integer Bessel function. After including the factor $k^2dk/d\epsilon_{\mathbf{k}}$, characterizing the density of states, the energy spectrum is given by $S(\epsilon_{\mathbf{k}},t)=k\Sigma_{l=0}^{\infty}|b_l(k,t)|^2$. The ionized part of the packet is

$$\psi(\mathbf{r},t)=\int d^3k\sum_{l=0}^{\infty}b_l(k,t)Y_{l0}(\hat{\mathbf{k}})\frac{1}{(\sqrt{2\pi})^3}\exp(i\mathbf{k}\cdot\mathbf{r}), \tag{5}$$

while the corresponding radial photoelectron distribution is given by

$$R(r,t)=\int|\psi(\mathbf{r},t)|^2r^2d\hat{\mathbf{r}}=\frac{2}{\pi}\sum_{l=0}^{\infty}r^2|X_l(r,t)|^2, \tag{6}$$

with $X_l(r,t)=\int_0^{\infty}b_l(k,t)j_l(kr)k^2dk$.

The applied approach based on calculating the transition amplitudes between the free states described in the length gauge, due to the interaction in the velocity gauge, is sometimes called ''a mixed gauge'' and is commonly used in the field. However, strictly speaking, it is proper to describe the evolution in terms of the projections of the system's wave function $\psi^V(t)$ calculated in the velocity gauge on the gauge-transformed final-state functions: $\exp[-i\mathbf{A}(t)\cdot\mathbf{r}]|1\rangle$ and $\exp[-i\mathbf{A}(t)\cdot\mathbf{r}]|\mathbf{k}\rangle$. Otherwise, one unwillingly takes into account a spike in the electric field due to an instantaneous switching off of the vector potential. For our smooth pulse, the problem does not appear at the beginning and at the end of the pulse. Thus, our probability amplitudes at time instants at which $A(t)\neq 0$ might be unreliable. To check the consequences of our using the mixed gauge we have estimated the value of the amplitude $\tilde{a}(t)\exp(-iE_1t)=\langle 1|\exp[i\mathbf{A}\cdot\mathbf{r}]|\psi^V(t)\rangle$ (which we cannot calculate exactly). If we now introduce into this formula the unit operator $I=|1\rangle\langle 1|+\int d^3k|\phi_{\mathbf{k}}\rangle\langle\phi_{\mathbf{k}}|$, where $|\phi_{\mathbf{k}}\rangle=|\psi_{\mathbf{k}}\rangle-|1\rangle\langle 1|\psi_{\mathbf{k}}\rangle$, $\psi_{\mathbf{k}}$ being the plane waves, and realize that our amplitudes $b_{\mathbf{k}}$ are in fact projections of the wave function onto the plane waves, we obtain

$$\tilde{a}(t)\exp(-iE_1t)=\langle 1|\exp[i\mathbf{A}(t)\cdot\mathbf{r}]|1\rangle a(t)\exp(-iE_1t)+\int d^3k\langle 1|\exp[i\mathbf{A}(t)\cdot\mathbf{r}]|\psi_{\mathbf{k}}\rangle b_{\mathbf{k}}(t)-\langle 1|\exp[i\mathbf{A}(t)\cdot\mathbf{r}]|1\rangle\int d^3k\langle 1|\psi_{\mathbf{k}}\rangle b_{\mathbf{k}}(t). \tag{7}$$

We have calculated the matrix elements in the above equation taking the bound-state function corresponding to the contact potential (and thus, not exactly to our bound-continuum coupling): $\psi_1(r)=\sqrt{\zeta/(2\pi)}\exp(-\zeta r)/r$. After the partial-wave expansion, one obtains

$$\tilde{a}(t)\exp(-iE_1t)=\frac{2\zeta}{A(t)}\arctan\frac{A(t)}{2\zeta}a(t)\exp(-iE_1t)+\sum_l\int d\epsilon_{\mathbf{k}}f_l[A(t),k]b_l(k,t)-\frac{4\zeta^{3/2}}{\pi^{1/2}A(t)}\arctan\frac{A(t)}{2\zeta}\int d\epsilon_{\mathbf{k}}\frac{k}{\zeta^2+k^2}\times b_0(k,t), \tag{8}$$

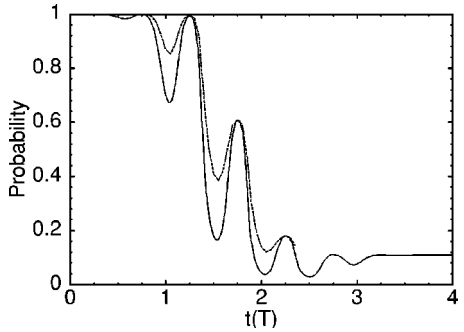

FIG. 1. The decay curve $|a(t)|^2$ of the initial-state population for $\epsilon_0=0.002$ a.u. and $\omega=0.004$ a.u. in the units of the field periods T; the broken line shows a fragment of the gauge-corrected decay curve $|\tilde{a}(t)|^2$. Note the maxima due to the electron's returning to the nucleus.

where

$$f_l[A(t),k]=\sqrt{\frac{(2l+1)\zeta}{\pi}}\frac{1}{A(t)}Q_l\left(\frac{\zeta^2+A^2+k^2}{2|A(t)|k}\right)c_l, \quad (9)$$

Q_l being the Legendre function of the second kind [15]; $c_l=-1$ for negative $A(t)$, and $c_l=(-1)^l$ for positive $A(t)$.

We have performed computations of the initial-state population $|a(t)|^2$, the photoelectron spectrum $S(\epsilon_{\mathbf{k}},t)$, and the radial density $R(r,t)$ for a "sine-square" pulse $A(t)=(\epsilon_0/\omega)\cos(\omega t)\sin^2(\pi t/\tau)$ of frequency $\omega=0.004$ a.u., intensity $\epsilon_0=0.002$ a.u., and duration $\tau=4T=4(2\pi/\omega)$. The corresponding Keldysh parameter is 0.47. The time evolution of the initial-state population is shown in Fig. 1. Note the deep minima of the population after an integer number of half cycles. The minima correspond to the moments at which the classical velocity of a particle under an influence of the laser electric field alone takes maximum or minimum values: it is then that the overlap of the wave packet with the initial state is the smallest. The maxima of the decay curve occur when the packet's velocity is zero; as we will see, the packet may then be quite a wide and multipeak structure, centered quite far from the nucleus, in fact, the packet's center may be localized close to a turning point. The broken curve in Fig. 1 shows the gauge-corrected decay probability $|\tilde{a}(t)|^2$. This curve differs quantitatively from the former one, but exhibits a qualitatively similar behavior, in particular, the maxima of the two curves coincide [they occur at the points at which $A(t)=0$], while the minima of the latter curve are somewhat more shallow. This means that our interpretation of the solid curve in terms of the electron being rescatttered is correct, in spite of the mixed-gauge approach.

In Fig. 2, we show the photoelectron spectrum. The solid curve shows the final spectrum (after four cycles, i.e., after the pulse has been switched off). It was sufficient to sum the angular momenta up to $l=32$. We observe a large number of peaks separated approximately by the photon energy ω, as in the standard ATI. The peaks, however, rise from a broad background typical of the tunneling regime, while their envelope has a local minimum. Note that the minimum is located at an energy smaller than the ponderomotive potential

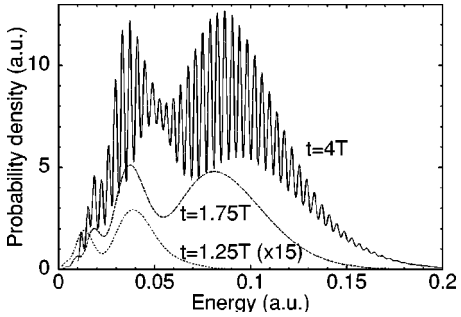

FIG. 2. The photoelectron energy spectrum $S(\epsilon_k,t)$ for $\epsilon_0=0.002$ a.u. and $\omega=0.004$ a.u., for $t=4$ T, solid line; $t=1.75$ T, broken line; $t=1.25$ T, dotted line (the latter results have been multiplied by a factor of 15). Note the minima in the envelope.

$U_P=\epsilon_0^2/(4\omega^2)$ (about 0.8 of its value), while in earlier observations [7–11], stress was put on the occurring of the minima or plateaux at energies of a few U_P. The other two curves in the figure show the spectrum at smaller times; such a spectrum would be obtained should the pulse be instantaneously switched off—the choice of the time instants at which $A(t)=0$ guarantees there are no artifacts due to the mixed gauge. Of course, the ATI peak structure can appear after a time long enough, so that the frequency should become well defined. The most important observation is that the most distinct minimum of the spectrum envelope about $\epsilon_{\mathbf{k}}=0.05$ a.u. is formed in the time interval preceding $t=1.75$ T, in which a significant part of the population is returning to the initial state. A less distinct minimum ($\epsilon_{\mathbf{k}}\approx 0.025$ a.u.) is connected with a return to the nucleus of a small but already noticeable part of the population about $t=1.25$ T.

The presence of a minimum in the energy spectrum implies that different parts of the packet are moving with different velocities. The packet must therefore be split into substructures (peaks or groups of peaks), which move away from each other. This is illustrated in Fig. 3, where we present the radial distribution of the packet. After the rescattering about 1.75 T we indeed observe two maxima in the envelope of the electron's radial distribution. A similar observation (on a low level of the population) is also observed

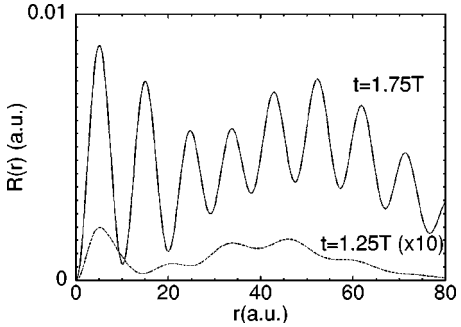

FIG. 3. The radial photoelectron distribution $R(r,t)$ for $\epsilon_0=0.002$ a.u. and $\omega=0.004$ a.u. after $t=1.75$ T, solid line; $t=1.25$ T, broken line (the latter results have been multiplied by a factor of 10). Note the minima in the envelope.

after 1.25 T. Our picture of the role of rescattering seems thus confirmed. Note that in this situation, any model based on a classical dynamics may be unreliable.

We have repeated the calculations for various values of the field frequency and intensity. The results were qualitatively similar. Again, the minimum in the spectrum envelope appeared at the time at which a significant part of the population has returned to the initial state, e.g., for $\epsilon_0 = 0.002$ a.u. and $\omega = 0.002$ a.u. the first significant minimum of $|a(t)|^2$ occurred already for $t \approx$ T and the structure in the peaks' envelope appeared before $t = 1.25$ T. For increasing field intensities, the minimum in the peaks' envelope is shifted towards larger energies (Fig. 4). This suggests that the described effects have no resonant character (cf. Ref. [8]). Changing $\cos\omega t$ into $\sin\omega t$ resulted, as expected, in a shift of the main events of the dynamics by a quarter of a cycle. We have also checked that the spectrum has a similar character in the case of a deeper potential well and that the minimum in the peaks' envelope is present also in the spectra corresponding to the particular partial waves, though the envelope is then somewhat less regular.

To conclude, let us stress that our quantum-mechanical study of the dynamics of photoionization for a three-dimensional model with a single active electron, in the regime lying on the border between the tunneling and the barrier suppression regimes, predicts the existence of a structure in the ATI peaks' envelope. Such a structure is here observed for energies being only a fraction of the ponderomotive potential U_P, while in works on HATI minima appeared for energies of a few U_P. It appears when a significant portion of the packet has been rescattered and is enriched due to consecutive returns to the nucleus. Our analysis of the decay of the initial-state population, energy spectra and the radial packet suggests that rescattering may indeed be responsible, not only for the extension of the spectrum beyond the value of the classical cutoff, but also for the details of its low-energy part.

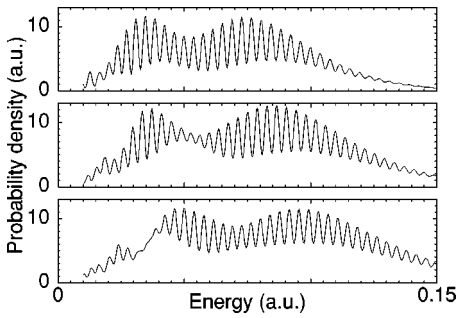

FIG. 4. The final photoelectron energy spectrum $S(\epsilon_k, 4\ \mathrm{T})$ for $\omega = 0.004$ a.u., for, top to bottom, $\epsilon_0 = 0.0018$ a.u., $\epsilon_0 = 0.0020$ a.u., and $\epsilon_0 = 0.0022$ a.u. Note the shift of the minimum in the envelope.

[1] M. Fedorov, *Atomic and Free Electrons in Strong Light Field* (World Scientific, Singapore, 1997).
[2] M. Protopapas, C.H. Keitel, and P.L. Knight, Rep. Prog. Phys. **60**, 389 (1997).
[3] G. Duchateau, G. Illescas, B. Pons, E. Cormier, and R. Gayet, J. Phys. B **33**, L571 (2000).
[4] D.W. Schumacher and P.H. Bucksbaum, Phys. Rev. A **54**, 4271 (1996).
[5] H.R. Reiss, Prog. Quantum Electron. **16**, 1 (1992).
[6] G.G. Paulus, W. Becker, W. Nicklich, and H. Walther, J. Phys. B **27**, L703 (1994).
[7] A. Lohr, M. Kleber, R. Kopold and W. Becker, Phys. Rev. A **55**, R4003 (1997).
[8] R. Kopold and W. Becker, J. Phys. B **32**, L419 (1999).
[9] G.G. Paulus, W. Nicklich, Huale Xu, P. Lambropoulos, and H. Walther, Phys. Rev. Lett. **72**, 2851 (1994).
[10] Bambi Hu, Jie Liu, and Shi-gang Chen, Phys. Lett. A **236**, 533 (1997).
[11] H.G. Muller and F.C. Kooiman, Phys. Rev. Lett. **81**, 1207 (1998).
[12] P. Bała, J. Matulewski, A. Raczyński, and J. Zaremba, Phys. Rev. A **57**, 4561 (1998).
[13] E.P. Wigner, Phys. Rev. **73**, 1002 (1948).
[14] A. Raczyński and J. Zaremba, J. Phys. B **29**, 449 (1996).
[15] M. Abramowitz and I. Stegun, *Handbook of Mathematical Functions* (Dover, New York, 1972).